Kinetic parameter estimation and fluctuation analysis of CO at SnO$_2$ single nanowires

Gerhard Tulzer[1,2]**, Stefan Baumgartner**[1,2]**, Elise Brunet**[1]**,**
Giorgio C Mutinati[1]**, Stephan Steinhauer**[1]**, Anton Köck**[1]**,**
Paolo E Barbano[3] **and Clemens Heitzinger**[1,4]

[1] AIT Austrian Institute of Technology, Donau-City-Strasse 1, A-1220 Vienna, Austria
[2] Department of Mathematics, University of Vienna, Nordbergstrasse 15, A-1090 Vienna, Austria
[3] Department of Mathematics, Yale University, New Haven, CT 06520-8283, USA
[4] Department of Applied Mathematics and Theoretical Physics (DAMTP), University of Cambridge, Wilberforce Road, Cambridge CB3 0WA, UK

E-mail: gerhard.tulzer.fl@ait.ac.at and C.Heitzinger@damtp.cam.ac.uk

Abstract
In this work, we present calculated numerical values for the kinetic parameters governing adsorption/desorption processes of carbon monoxide at tin dioxide single-nanowire gas sensors. The response of such sensors to pulses of 50 ppm carbon monoxide in nitrogen is investigated at different temperatures to extract the desired information. A rate-equation approach is used to model the reaction kinetics, which results in the problem of determining coefficients in a coupled system of nonlinear ordinary differential equations. The numerical values are computed by inverse-modeling techniques and are then used to simulate the sensor response. With our model, the dynamic response of the sensor due to the gas–surface interaction can be studied in order to find the optimal setup for detection, which is an important step towards selectivity of these devices. We additionally investigate the noise in the current through the nanowire and its changes due to the presence of carbon monoxide in the sensor environment. Here, we propose the use of a wavelet transform to decompose the signal and analyze the noise in the experimental data. This method indicates that some fluctuations are specific for the gas species investigated here.

(Some figures may appear in colour only in the online journal)

1. Introduction

Gas sensors have applications in various fields ranging from industrial process control and personal safety to environmental monitoring. Early and reliable diagnosis of diseases, air quality monitoring in heating, ventilating, and air conditioning (HVAC), or alert systems for carbon monoxide in household heating systems are examples of applications requiring reliable, compact, and efficient gas-sensor systems. Metal-oxide semiconductors are very promising materials to develop such gas sensors; in particular, SnO$_2$, ZnO, TiO$_2$, In$_2$O$_3$, WO$_3$, and CuO have been thoroughly investigated in the past decades. Tin dioxide (SnO$_2$) has been the most

prominent sensing material because of its high sensitivity to a broad range of gas species. A variety of gas-sensor devices based on SnO$_2$ thin films have been realized [1–4]. The advantages of nanowires over thin films, such as the higher surface-to-volume ratio and higher crystalline quality have encouraged the development of gas sensors based on SnO$_2$ nanobelts and nanowires as sensing elements, as reported in [5–12]. The gases detected by SnO$_2$ nanowire sensors are numerous (CO, ethanol, H$_2$, H$_2$S, NO$_2$, NH$_2$, etc). The concentration range as well as the corresponding sensitivity values for the detection of several target gases by SnO$_2$ nanowire sensors have been reviewed in [13].

Still selectivity remains a crucial issue. One approach to remedy missing selectivity is functionalization of the surface, which either inhibits or favors the occurrence of certain reactions. Nonetheless, there is still no general quantitative understanding of the sensor responses, not even taking functionalizations of the sensor into account. Computer simulations are an advantageous tool for obtaining accurate answers to these qualitative as well as quantitative questions. The first step in a rigorous carrier-transport investigation is the study of the processes taking place at the sensor surface. It is necessary to determine the crucial parameters of the different gas–surface interactions, such as the kinetic parameters, to reveal the characteristic sensor response with respect to a certain gas.

The nanowires used in this work are monocrystalline. The advantage of monocrystalline devices compared to polycrystalline ones are better defined structures and behavior. Our simulation approach here is similar to the physics based modeling of nanowire field-effect biosensors [14–18]. The processes determining the charge concentration in the boundary layer at the sensor surface need to be understood and quantified in order to be able to optimize sensor designs [16, 19, 20]. Therefore this work focuses on the modeling of the surface reactions.

Although there are a number of computational investigations of the sensor signal due to constant concentrations of carbon monoxide (CO), hydrogen (H_2), or humid air being present in the atmosphere [21–23], the modeling of the response to gas pulses is just evolving [24]. Recent studies [21] argued that, contrary to prior assumptions, CO does mainly interact with the nanowire lattice and that the reaction with pre-adsorbed oxygen is only a side effect. It seems straightforward to eliminate these side effects and just consider the main reaction. As a consequence, this work deals with measuring the dynamic response of single SnO_2 nanowire sensors to CO in nitrogen (N_2), and from the experimental results we estimate numerical values for the kinetic parameters during exposure to low concentrations of CO in the inert atmosphere and also investigate their dependence on temperature. This approach provides insight into the dynamic behavior of the semiconductor nanowire and also enables an estimation of the parameters in each reaction step by step.

Additionally, the noise in the current through the nanowires is investigated. A time–frequency analysis of the signal is performed with an emphasis on comparing the two cases with and without CO. The motivation is to extract additional information from the noise inherent in the signal in order to alleviate the problems of sensor drift and of the missing selectivity. We show that the derivative of the voltage correlates with certain high-frequency components of the signal.

This study is organized as follows: detailed information on the sensor preparation and the equipment used is given in section 2. We describe the surface-reaction model in section 3. In section 4, we present the parameter-estimation procedure including a description of the experimental conditions investigated. The estimation results are discussed in section 5.

Finally, the wavelet analysis of the signal is presented in section 6.

## 2. Experimental section

2.1. Methods

The synthesis of SnO_2 nanowires is a two-step process. First, an SnO_2 thin film is deposited on a Si-substrate with a thickness of $\approx$300 nm by spray pyrolysis (details reported in [25]). In the second step, the SnO_2 coated Si-substrate is introduced in a tube furnace and a second SiO_2/Si substrate coated with 40 nm Cu by sputtering is stacked on top of the first substrate face down. The two substrates are separated by spacers, which are about 750 μm high. The furnace is heated from room temperature to 900 °C for 2.5 h with a constant argon flow of 1000 sccm. The SnO_2 nanowires grown on the top Cu-coated substrate are transferred by ultrasonication of the substrate in isopropanol and successive spin-coating of the solution on a thermally oxidized (300 nm SiO_2) silicon chip. A single photolithography process step followed by the evaporation of Ti–Au contact pads (thickness of 10 nm and 150 nm, respectively) and a final lift-off process complete the fabrication of the single SnO_2 nanowire sensors.

The nanowire-based gas sensors are glued on microheater elements (10 × 2 Pt 6.8–0.4, Delta-R GmbH) and a Pt100 temperature sensor (4 × 1 Pt 100B, Delta-R GmbH). This specific setup enables one to heat the sensors up to a temperature of 400 °C and to simultaneously control the temperature. The sensors are finally bonded to a ceramic carrier and mounted in the gas measurement chamber. A constant current of 50 nA is applied to the single-nanowire sensor and the voltage is measured by a Keithley 2400 SourceMeter.

The sensing performance of the sensor devices is investigated in an automated measurement setup, which allows precise adjustment of the gaseous environment. Nitrogen (Linde Gas) is used as background gas. The test gas is a ready-made mixture of CO (900 ppm) in nitrogen (Linde Gas), which is mixed to the background gas in a gas mixing vessel. The total flow rate of gas (N_2 or N_2 plus CO) is controlled by mass flow controllers (MFCs) and is always kept constant at 1000 sccm. The measurements are performed in dry conditions.

2.2. Results

Figure 1(a) shows a SEM image of the dense interlacing of SnO_2 nanowires as grown on the top Cu-coated substrate. The SnO_2 nanowires have diameters in the range of 40–300 nm and lengths up to hundreds of micrometers. The SnO_2 nanowire, which has been measured in different gaseous environments, has a diameter of 265 nm and exhibits a length of 53 μm between the two Ti–Au contact pads, as shown in figure 2. TEM analyses have been performed in order to characterize the crystalline structure of the nanowires. Bright-field images and electron-diffraction patterns were acquired using a Tecnai F20 with a field-emission gun (FEG)
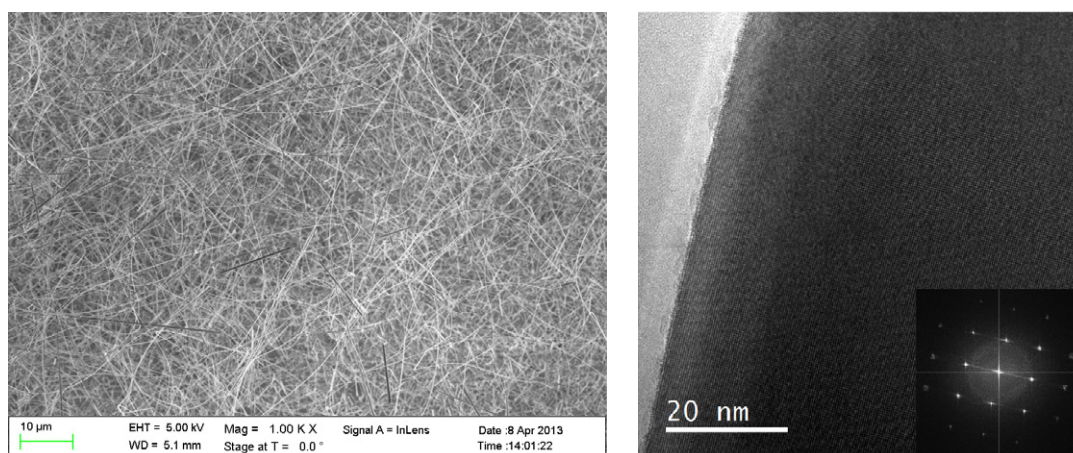
Figure 1. Left: SEM image of the dense interlacing of SnO$_2$ nanowires as grown on the top Cu-coated substrate. Right: high-resolution TEM image of a monocrystalline SnO$_2$ nanowire and the corresponding electron-diffraction pattern.
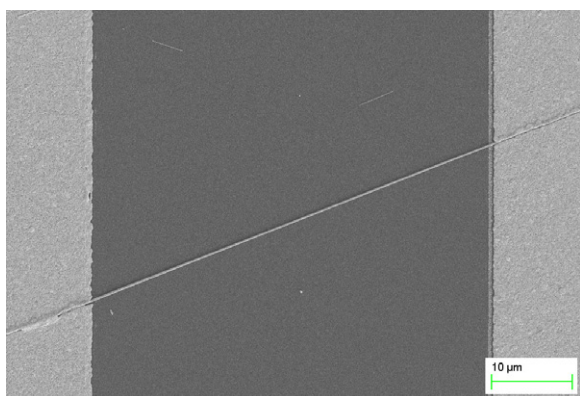
Figure 2. SEM image of the measured single-nanowire sensor. The SnO$_2$ nanowire is contacted by Ti–Au contact pads visible on the left- and right-hand sides.

operating at 200 kV. The microscope has a post-column energy filter (Gatan Imaging Filter, GIF) and the images were recorded in zero-loss filtered mode, using a 10 eV wide slit (i.e. elastically scattered electrons only).

Figure 1(b) shows a high-resolution TEM image and the corresponding electron-diffraction pattern (inset) of a typical SnO$_2$ nanowire fabricated using this process. The structure of the nanowire is clearly monocrystalline. Several SnO$_2$ nanowires have been investigated and all present a monocrystalline structure. A more complete discussion of the crystalline structure of the SnO$_2$ nanowires can be found in [26].

The change of resistance of the SnO$_2$ single nanowire shown in figure 2 is investigated in an inert atmosphere (N$_2$) and in an environment composed of CO in N$_2$. Figure 3 shows the influence of the temperature on the resistance of the SnO$_2$ nanowire measured in N$_2$. The sensor has been operated for 90 min at each temperature ranging from 250 to 350 °C in steps of 25 °C. The resistance of the SnO$_2$ nanowire increases with increasing temperature. The value of the electrical resistance of the SnO$_2$ nanowire reaches 3.5 MΩ at 250 °C, 4.1 MΩ at 300 °C, and 4.5 MΩ at 350 °C. It is

noticed that the resistance values at 250 °C and 300 °C during the cooling phase are higher than during the heating phase: 3.9 MΩ and 4.3 MΩ, respectively.

Figure 4 shows the change of resistance of the single SnO$_2$ nanowire in the presence of a mixed atmosphere of CO and N$_2$ in comparison to pure N$_2$. The nanowire sensor is first measured in pure N$_2$ for 60 min at 300 °C. A flow of CO—corresponding to a concentration of 50 ppm—is mixed with the N$_2$ flow and introduced into the gas measurement chamber for 15 min. Afterwards the CO flow is switched off for 15 min and the environment in the gas measurement chamber is composed of pure N$_2$. This CO pulse is repeated a second time. The same measurement run is repeated at 350 °C with a first heating step in pure N$_2$ of 90 min. The resistance of the SnO$_2$ nanowire decreases in the presence of CO, with a resistance drop (ratio of the resistance in N$_2$ and the resistance in CO) of 1.07 and 1.075 for the first pulse of CO at 300 °C and 350 °C, respectively.

2.3. Discussion

Figure 3 shows that the resistance of the SnO$_2$ nanowire increases with increasing temperature, which is not expected for a semiconducting material. The drift in the resistance occurring during time intervals of constant temperature is due to the occupation of the intrinsic surface state, which is a very slow process [27]. This is discussed in detail in section 5.1.

Regarding the difference in the resistance values at 250 and 300 °C during the heating phase and the cooling phase, it must be noted that the equilibrium has not been attained before temperature changes. Extrapolating the measured resistance at 250 °C in the heating phase (from 0 to 80 min) and cooling phase (from 470 to 500 min) and likewise at 300 °C for the steps in the ranges from 170 to 260 min and from 450 to 470 min yields differences in resistance smaller than 1%, indicating a good stability of the nanowire conductivity and no hysteresis.

Figure 4 shows the response of the SnO$_2$ single-nanowire sensor to 50 ppm CO in dry N$_2$ atmosphere. The resistance
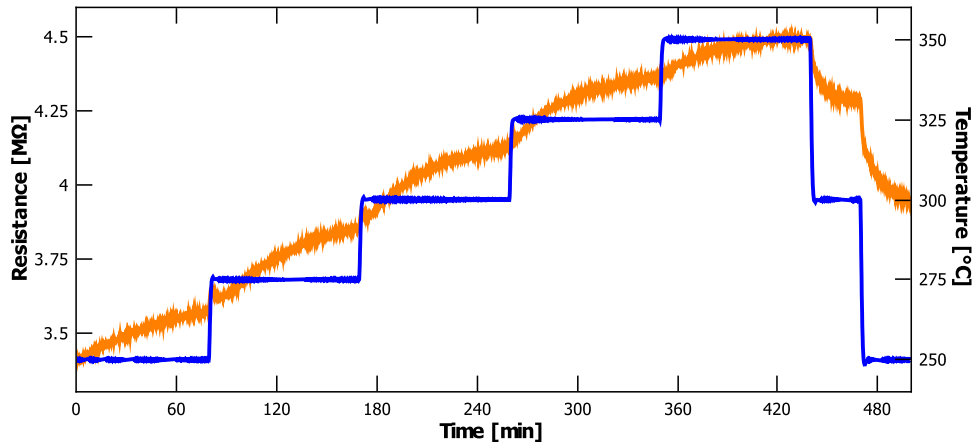
Figure 3. Measured resistance (orange) and measured temperature profile (blue) in a pure nitrogen atmosphere.
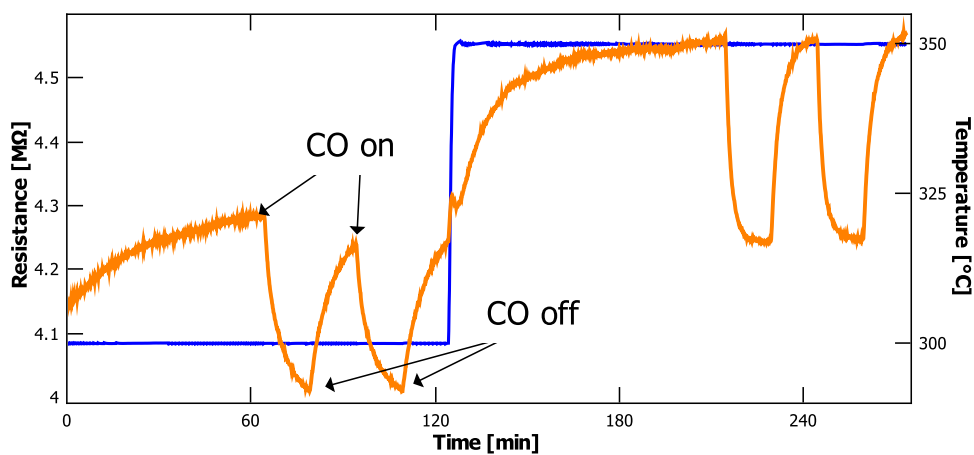
Figure 4. Measured resistance (orange) and measured temperature profile (blue). The CO pulses are indicated in the picture.

decreases in the presence of CO, which is in agreement with the reaction mechanism proposed in the literature [28] and discussed later in section 3.2. The CO adsorption process at the surface of the SnO_2 nanowire is a reversible process, as demonstrated by the increase of resistance back to its initial value after the CO flow has been switched off. The measurement of CO in N_2 is crucial for the establishment of the kinetic parameters governing the adsorption/desorption processes of CO at the SnO_2 nanowire sensor.

3. The model

The sensing principle is based on the relation between the electrical conductance of the semiconductor and the surrounding gas. The conductance of the sensor is influenced mainly by the temperature and the electrical potential inside the nanowire, which itself depends on the surface charge. Since the adsorption of gas molecules leads to an electron transfer which changes the surface charge, information on the surface charge and hence the gas species is obtained by conductometric experiments.

To describe the gas adsorption process for the computation of the surface potential, a rate-equation approach [29] is used, leading to a system of highly

nonlinear ordinary differential equations (ODEs). The kinetic parameters of the surface reactions arise as coefficients in the ODE system. Therefore, the objective is to determine their numerical values in order to obtain quantitative insights and simulate the sensor behavior under various conditions.

3.1. Linking surface effects to conductance changes

The nanowire conductance depends on the surface-charge density and is—according to potential barrier theory—given by [30]

$$G = G_0 T^{-\frac{3}{2}} e^{-\frac{qV_S}{k_B T}}, \tag{1}$$

where G_0 is a constant factor taking into account the geometry of the nanowire, the bulk electron density and the electron mobility in the SnO_2 nanowire, q is the elementary charge, V_S is the surface potential, k_B is the Boltzmann constant, and T is the temperature in kelvin. The exponential term describes the decrease of the electron density due to the electric potential in the nanowire that is generated by surface charges.

To compute the surface potential, we use a surface-state model that considers physisorption and chemisorption (as well as their inverse reactions) as the processes taking place at

the sensor surface. Hence the effective surface-charge density N_{SS} is given by a superposition of the charge density due to occupied surface states stemming from the interaction of the electrons in the nanowire and those stemming from the interaction of target gases with the surface. The surface potential and the surface-state density are linked via the relationship [31]

$$V_S = \frac{q N_{SS}^2}{2\epsilon \epsilon_0 N_D},\tag{2}$$

where ϵ_0 is the dielectricity constant, ϵ is the relative permittivity of tin dioxide, and N_D is the density of ionized donors.

3.2. Sensor behavior in an inert atmosphere and response to carbon monoxide

The dynamics of the intrinsic state occupation are described by the chemical reaction [27]

$$S_{i,u} + e^- \Longleftrightarrow S_{i,o},\tag{3}$$
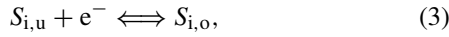
where S_i denotes an intrinsic surface state and the indices u and o denote if it is unoccupied or occupied. In case the atmosphere is inert (e.g., a nitrogen atmosphere), this is the only reaction.

If CO is present in an inert atmosphere, literature [28] proposes the reaction mechanism

$$CO + S_{e,u} \Longleftrightarrow [CO{-}S_e],\tag{4}$$

$$[CO - S_e] \Longleftrightarrow [CO^+ - S_e] + e^-,\tag{5}$$
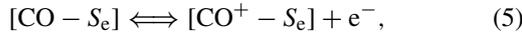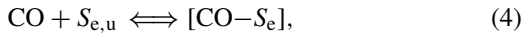
where S_e denotes an extrinsic surface state. Note that since an electron is released into the nanowire in this case, the surface states are positively charged, while the intrinsic ones are negatively charged.

The mass-action law provides expressions for the change of the densities of the respective surface species. Hence we obtain the coupled system of nonlinear ordinary differential equations

$$\frac{dN_i}{dt} = k_1 e^{-\frac{E_1}{k_B T}} n_S [S_{i,u}] - k_2 e^{-\frac{E_2}{k_B T}} N_i,\tag{6a}$$

$$\frac{dN_{CO}}{dt} = k_3 e^{-\frac{E_3}{k_B T}} [S_{e,u}][CO] - k_4 e^{-\frac{E_4}{k_B T}} N_{CO}$$
$$- \frac{dN_{CO^+}}{dt},\tag{6b}$$

$$\frac{dN_{CO^+}}{dt} = k_5 e^{-\frac{E_5}{k_B T}} N_{CO} - k_6 e^{-\frac{E_6}{k_B T}} n_S N_{CO^+},\tag{6c}$$

where k_i is a frequency factor, E_i is an activation energy,

$$[S_{i,u}] := S_i - N_i$$

is the density of unoccupied intrinsic surface states, and

$$[S_{e,u}] := S_e - N_{CO} - N_{CO^+} = S_e - N_e$$

is the density of unoccupied extrinsic surface states. The quantity $N_\#$ denotes the density of species #. The expression

$$n_S := N_D e^{-\frac{q^2 N_{SS}^2}{2\epsilon \epsilon_0 N_D k_B T}}\tag{7}$$

represents the density of electrons that can reach the nanowire surface [27, 31]. In this case, we have $N_{SS} = N_i - N_{CO^+}$ because of opposite charges of the states. The reaction constants

$$k_i e^{-E_i/k_B T} =: \kappa_i$$

are already written in the Arrhenius form to respect their temperature dependence.

4. Determination of the parameters

4.1. Non-dimensionalization and scaling

In order to simplify the equations and also to stabilize the numeric procedure, we need dimensionless and properly scaled variables. We therefore substitute (as in [27])

$$\widetilde{N}_\# := \frac{N_\#}{N_D^{2/3}}, \qquad \widetilde{S}_\# := \frac{S_\#}{N_D^{2/3}}, \qquad \widetilde{T} := \frac{\epsilon_0 k_B}{q^2 N_D^{1/3}} T,$$

where # denotes any index. Condensing some constants and parameters and, by abusing notation, writing the dimensionless variables without a tilde again for the sake of simplicity, we finally arrive at

$$N_i' = \alpha_1 e^{-\frac{\lambda_1}{T}} e^{-\frac{N_{SS}^2}{2\epsilon T}} (S_i - N_i) - \alpha_2 e^{-\frac{\lambda_2}{T}} N_i,\tag{8a}$$

$$N_{CO}' = \alpha_3 e^{-\frac{\lambda_3}{T}} (S_e - N_e)[CO] - \alpha_4 e^{-\frac{\lambda_4}{T}} N_{CO} - N_{CO^+}',\tag{8b}$$

$$N_{CO^+}' = \alpha_5 e^{-\frac{\lambda_5}{T}} N_{CO} - \alpha_6 e^{-\frac{\lambda_6}{T}} e^{\frac{N_{SS}^2}{2\epsilon T}} N_{CO^+}.\tag{8c}$$

The goal is to determine the parameters $\{\alpha_i\}_{i=1,\dots,6}$, $\{\lambda_i\}_{i=1,\dots,6}$, and the densities S_i and S_e of the available intrinsic and extrinsic surface states.

4.2. Determination procedure

As described in section 2, two measurements have been performed: first, the change of conductance of the SnO_2 nanowire sensor has been investigated in an inert N_2 atmosphere at different temperatures in the range from 250 to 350 °C (figure 3), then 50 ppm CO has been periodically added to the N_2 atmosphere at 300 and 350 °C (figure 4).

From the first measurement in an inert atmosphere (pure N_2), the parameters for the intrinsic surface-state occupation are determined. The numerical values obtained are fixed and they are then used to determine the parameters governing CO adsorption. From the second measurement in a partly mixed atmosphere of CO and N_2, the remaining parameters for CO adsorption are determined.

By determining the reaction parameters in two steps, the computation times are reduced significantly while the accuracy is improved as well. The values of the reaction parameters are computed using our code in the *Mathematica* environment. To this end, the system (8) is solved numerically depending on the parameters and the solution is compared to the time evolution of the sensor signal. The deviation of the numerical solution from the measured time series is
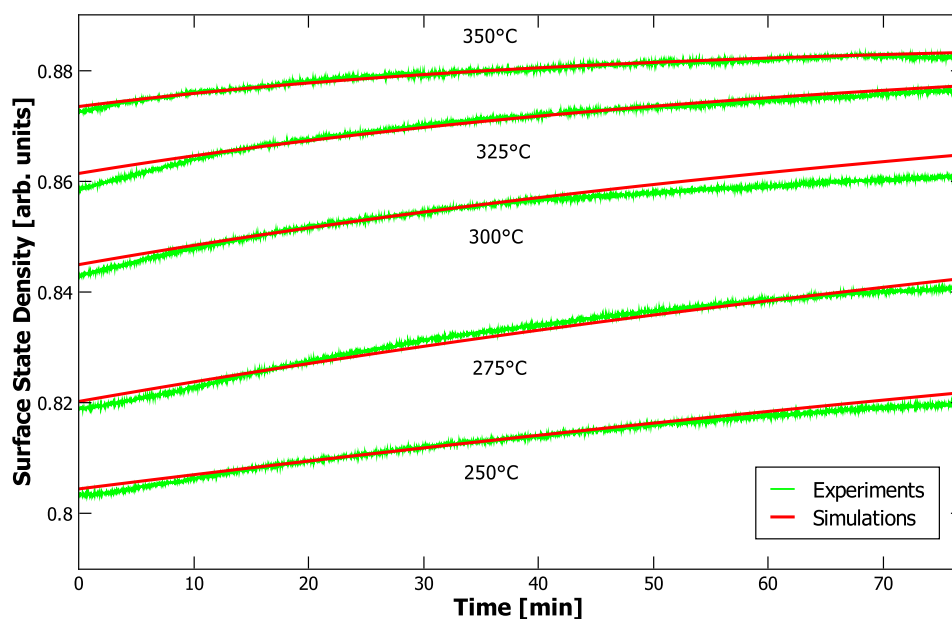
Figure 5. Measurements and simulation of a nanowire sensor in the N$_2$ atmosphere during the heating phase.

minimized with respect to the L^2-norm using a simulated-annealing algorithm.

Since there is a slight uncertainty in the sensor signal during and right after a heating process as the location of the sensor does not exactly coincide with the location of temperature sensor and the heating element, the initial conditions for the simulation are chosen at a point where all components of the system have reached thermal equilibrium. In this manner, the accuracy can be improved significantly.

5. Results and discussion

5.1. Inert atmosphere

The sensor behavior in the N$_2$ atmosphere was investigated at 250, 275, 300, 325, and 350 °C according to the temperature profile shown in figure 3. The experimental results indicate that the variation of the intrinsic surface states is very slow (time constants of minutes), which was also reported in [22, 27]. Interestingly, the variation is much faster when the sensor is cooled down to a fixed temperature instead of heated up. This fact is also indicated by the estimated numerical values for the reaction constants κ_i, which are orders of magnitude higher for the drift after cooling than after heating (see table 1). This fact can be exploited for time-saving measurement strategies.

For each case, the simulations using the estimated parameters agree very well with the experimental data at all investigated temperatures, as can be seen in figures 5 and 6. This also confirms the investigated reaction paths.

5.2. Carbon monoxide in inert atmosphere

For the estimation of the parameters of the CO adsorption process, the numerical values of the parameters in equation (8a)

Table 1. Parameters for increasing and decreasing temperature steps in the N$_2$ atmosphere.

Parameter	Increasing steps	Decreasing steps
α_1	85 552	504 550
α_2	223.86	100.56
λ_1	0.3501	0.3150
λ_2	0.7289	0.1764
S_i	0.8855	0.9176

Table 2. Parameters for CO pulses.

Parameter	Value
α_3	1.0509×10^6
α_4	5.8091×10^{12}
α_5	3.8439×10^{21}
α_6	3.0745×10^{13}
S_e	72.411
λ_3	0.2932
λ_4	0.8271
λ_5	1.4551
λ_6	0.8448

were set to those already found and shown in table 1. Then the values of $\{\alpha_i\}_{i=3,...,6}$, $\{\lambda_i\}_{i=3,...,6}$, and S_e were calculated and are shown in table 2. Since these values are again much higher than the values governing the intrinsic sensor behavior, it is obvious that the response to CO is fast compared to the change of the intrinsic states after a temperature change.

The qualitative behavior of the nanowire is reproduced very well at both temperatures, as can be seen from figure 7. The difference between simulation and measurement is small enough to be negligible at 350 °C. However, there is a difference at 300 °C, which is most likely due to a small linear drift in the average sensor signal that can be observed in this interval of the measurement. Nevertheless, the maximal
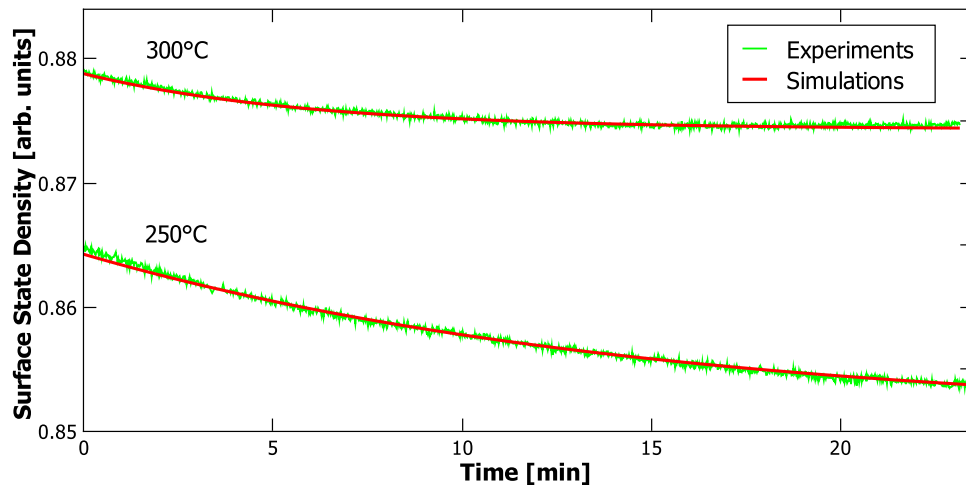
Figure 6. Measurements and simulation of a nanowire in the N$_2$ atmosphere during the cooling phase.
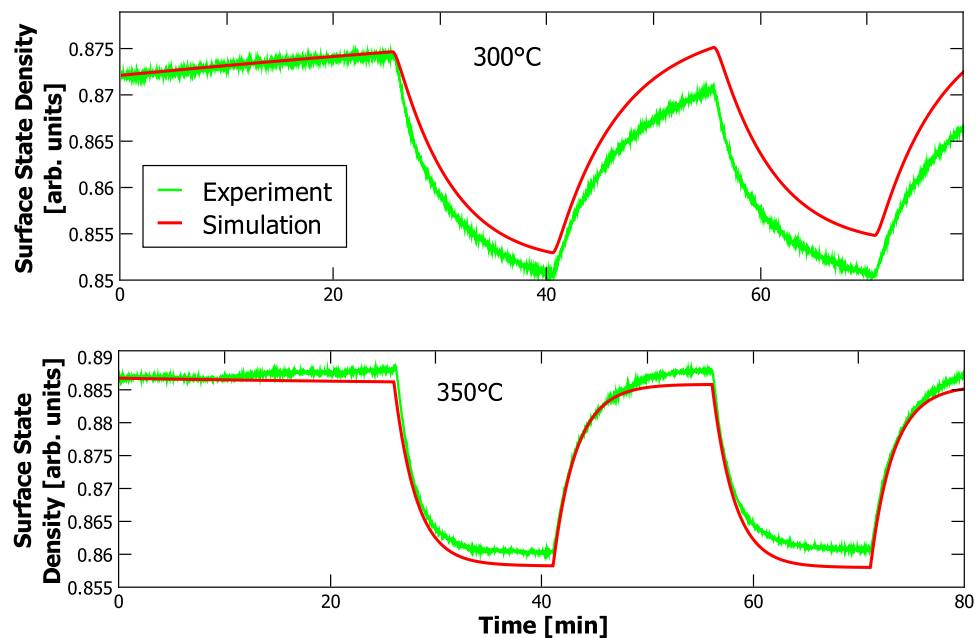
Figure 7. Measurements and simulation for CO pulses at 300 °C (top) and 350 °C (bottom).

difference between measurement and simulation is smaller than 1%.

The investigated model is a quantitative approach to understand the processes taking place at the sensor surface. Although the parameter determination is a delicate task due to the nonlinearity of the equations, it is unlikely that this model can be simplified any further to lower the computational cost.

6. Wavelet analysis

The time series including gas pulses investigated here consists of 72 459 time-samples of the voltage. Figure 8 shows a decomposition of the voltage signal s into components a_5 and d_i, $i \in \{1, \ldots, 5\}$, using Meyer wavelets such that the equation

$$s = a_5 + \sum_{i=1}^{5} d_i$$

holds. The vector a_5 denotes the average response, whereas the vectors d_i, $i \in \{1, \ldots, 5\}$, contain the higher-frequency components. This approach is local in time and hence advantageous for the analysis of transient signals compared to Fourier analysis.

It is interesting to note that the component d_5—and to a lesser extent the component d_4—is clearly related to the time derivative of the signal. On the other hand, this dependency is not observed in the components d_1, d_2, and d_3. This fact suggests a measurement strategy circumventing sensor drift.

It is instructive to compare the two cases where only N$_2$ and where both N$_2$ and CO are present in the sensor atmosphere. Figure 9 shows the case when only N$_2$ is present, whereas figure 10 shows the case when both N$_2$ and CO are present. It is found that the response of the nanowire in the second case with CO is much more regular in the sense that the global variance of the high frequencies is much lower. The
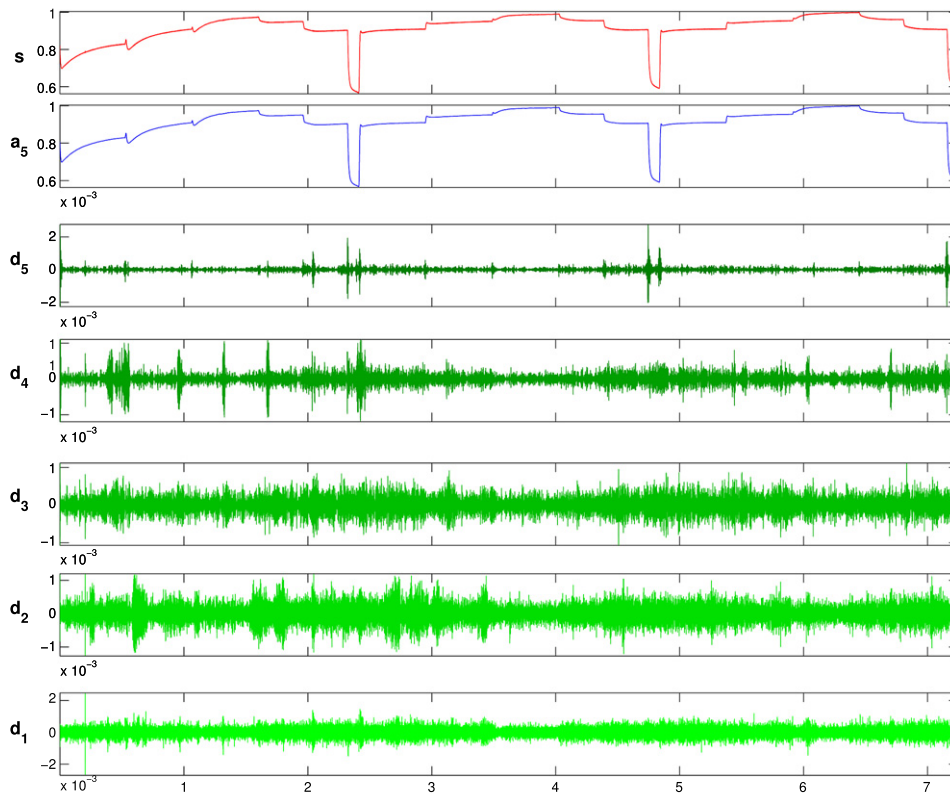
Figure 8. Decomposition of the voltage signal using Meyer wavelets.
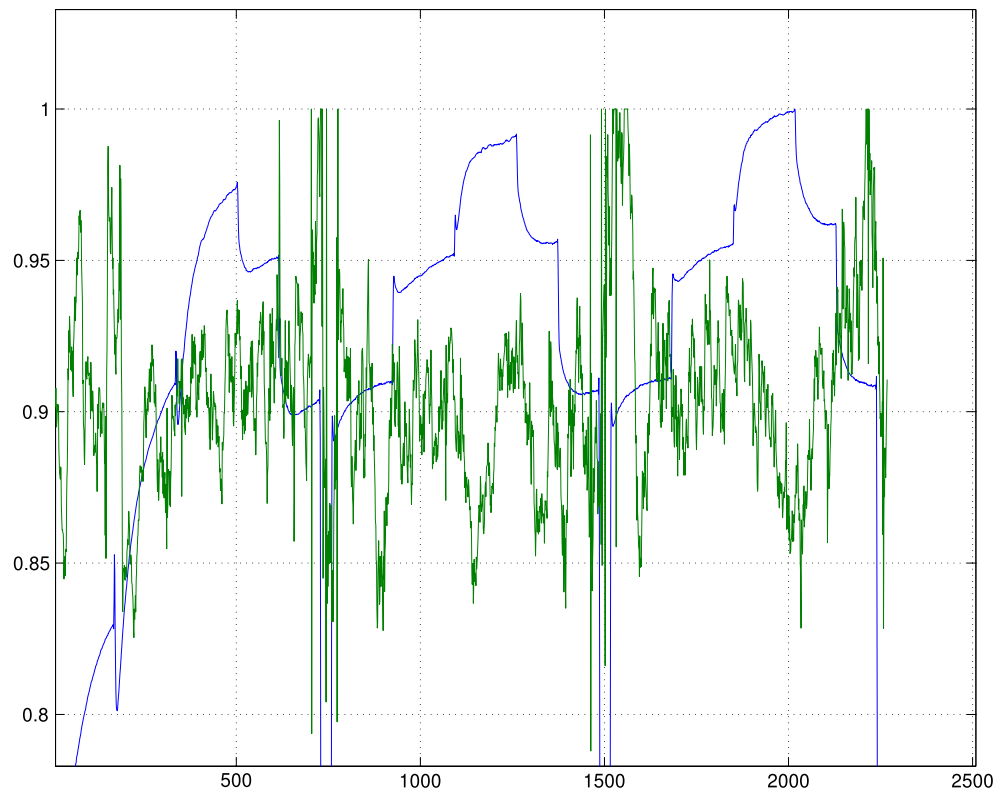
Figure 9. Detail of one of the high-frequency bands when only N_2 is present in the sensor atmosphere.

amplitudes of the high-frequency coefficients are shown in green in figures 9 and 10, being much lower in the second case in figure 10. This difference in the fluctuations suggests that certain characteristics of the fluctuations are specific to the gas species, and furthermore this suggests a strategy for discerning between gas species. The different behavior of the
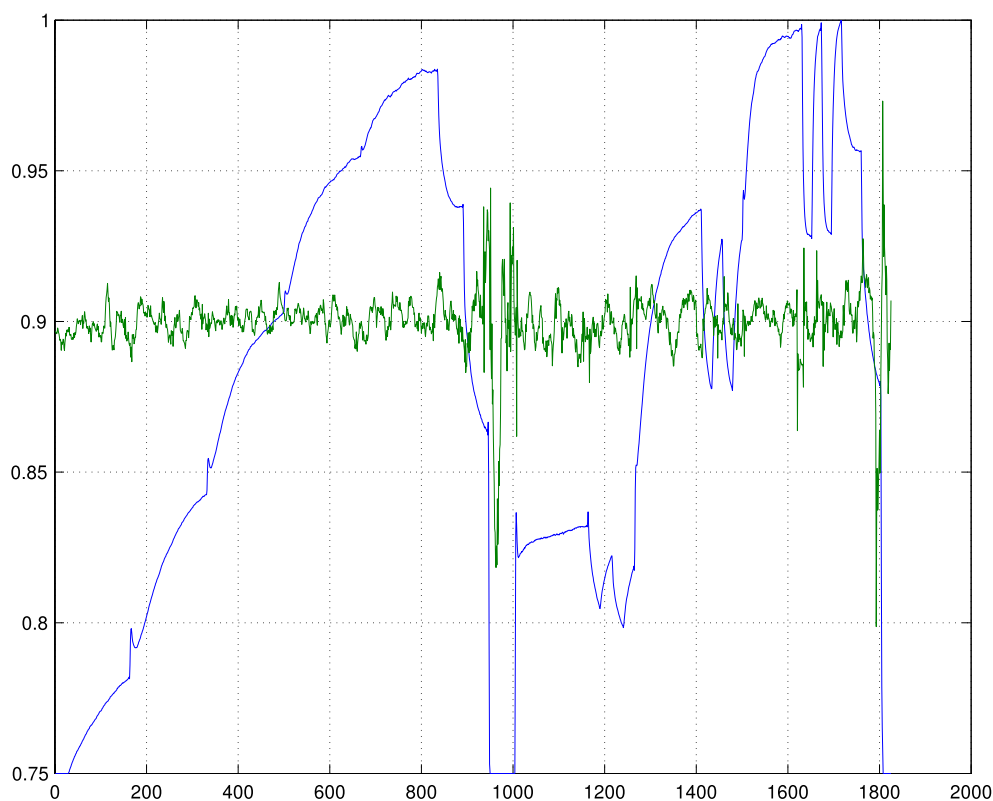
Figure 10. Detail of one of the high-frequency bands when both N_2 and CO are present in the sensor atmosphere.

high-frequency components can be understood in terms of the different coefficients in the stochastic equations describing the reactions of the gas species at the monocrystalline nanowire surfaces.

7. Conclusions

We have used a rate-equation approach for the adsorption/desorption processes at SnO_2 nanowire surfaces in order to quantitatively characterize the sensor behavior under inert conditions and with CO presence in the N_2 atmosphere. To this end, we calculated the governing kinetic parameters and also investigated their temperature dependence, since temperature variation is believed to be a strategy for identifying different gases. The temperature range investigated here is compatible with highly integrated CMOS devices. The drift over time of the sensor signal after heating and cooling periods has been found to be very small. Finally, the simulation of the sensor behavior agrees very well with the experimental data and indicates that the relevant reaction paths have been identified and included quantitatively.

Additionally, we have investigated the fluctuations in the monocrystalline nanowires depending on the sensor atmosphere. It was found that the derivative of the voltage signal correlates with certain high-frequency components of the signal, and it was also found that the amplitude of high-frequency coefficients is considerably lower during CO pulses. These findings, together with the kinetic model of the gas–surface interactions, provide important insight towards theoretical understanding of monocrystalline nanowires for

gas sensing and are crucial for further research on the selectivity of such devices.

References

[1] Meixner H, Gerblinger J, Lampe U and Fleischer M 1995 Thin-film gas sensors based on semiconducting metal oxides *Sensors Actuators* B **23** 119–25

[2] Korotcenkov G 2007 Metal oxides for solid-state gas sensors: what determines our choice? *Mater. Sci. Eng.* B **139** 1–23

[3] Wang C, Yin L, Zhang L, Xiang D and Gao R 2010 Metal oxide gas sensors: sensitivity and influencing factors *Sensors* **10** 2088–106

[4] Zhou D, Gan L, Gong S, Fu Q and Liu H 2011 p-type metal oxide doped SnO_2 thin films for H_2S detection *Sensor Lett.* **9** 651–4

[5] Kolmakov A, Klenov D O, Lilach Y, Stemmer S and Moskovits M 2005 Enhanced gas sensing by individual SnO_2 nanowires and nanobelts functionalized with Pd catalyst particles *Nano Lett.* **5** 667–73

[6] Comini E 2006 Metal oxide nano-crystals for gas sensing *Anal. Chim. Acta* **568** 28–40

[7] Ahn M W, Park K S, Heo J H, Park J G, Kim D W, Choi K J, Lee J H and Hong S H 2008 Gas sensing properties of defect-controlled ZnO-nanowire gas sensor *Appl. Phys. Lett.* **93** 263103

[8] Choi Y J, Hwang I S, Park J G, Choi K J, Park J H and Lee J H 2008 Novel fabrication of an SnO_2 nanowire gas sensor with high sensitivity *Nanotechnology* **19** 095508

[9] Hernandez-Ramirez F, Prades J D, Hackner A, Fischer T, Mueller G, Mathur S and Morante J R 2011 Miniaturized ionization gas sensors from single metal oxide nanowires *Nanoscale* **3** 630–4

[10] Dattoli E N, Davydov A V and Benkstein K D 2012 Tin oxide nanowire sensor with integrated temperature and gate control for multi-gas recognition *Nanoscale* **4** 1760–9

[11] Hunt H and Armani A 2010 Label-free biological and chemical sensors *Nanoscale* **2** 1544–59

[12] Brunet E, Maier T, Mutinati G C, Steinhauer S, Köck A, Gspan C and Grogger W 2012 Comparison of the gas sensing performance of SnO_2 thin film and SnO_2 nanowire sensors *Sensors Actuators* B **165** 110–8

[13] Arafat M M, Dinan B, Akbar S A and Haseeb A S M A 2012 Gas sensors based on one-dimensional nanostructured metal-oxides: a review *Sensors* **12** 7207–58

[14] Heitzinger C, Mauser N and Ringhofer C 2010 Multiscale modeling of planar and nanowire field-effect biosensors *SIAM J. Appl. Math.* **70** 1634–54

[15] Bulyha A and Heitzinger C 2011 An algorithm for three-dimensional Monte-Carlo simulation of charge distribution at biofunctionalized surfaces *Nanoscale* **3** 1608–17

[16] Baumgartner S, Vasicek M, Bulyha A and Heitzinger C 2011 Optimization of nanowire DNA sensor sensitivity using self-consistent simulation *Nanotechnology* **22** 425503

[17] Punzet M, Baurecht D, Varga F, Karlic H and Heitzinger C 2012 Determination of surface concentrations of individual molecule-layers used in nanoscale biosensors by *in-situ* ATR–FTIR spectroscopy *Nanoscale* **4** 2431–8

[18] Baumgartner S and Heitzinger C 2012 Existence and local uniqueness for 3D self-consistent multiscale models of field-effect sensors *Commun. Math. Sci.* **10** 693–716

[19] Baumgartner S, Vasicek M and Heitzinger C 2012 Modeling and simulation of nanowire based field-effect biosensors

[20] Baumgartner S, Heitzinger C, Vacic A and Reed M A 2013 Predictive simulations and optimization of nanowire field-effect PSA sensors including screening *Nanotechnology* **24** 225503

[21] Fort A, Mugnaini M, Rocchi S, Serrano-Santos M B, Vignoli V and Spinicci R 2007 Simplified models for SnO_2 sensors during chemical and thermal transients in mixtures of inert, oxidizing and reducing gases *Sensors Actuators* B **124** 245–59

[22] Fort A, Mugnaini M, Rocchi S, Vignoli V, Comini E, Faglia G and Ponzoni A 2010 Metal-oxide nanowire sensors for CO detection: characterization and modeling *Sensors Actuators* B **148** 283–91

[23] Fort A, Mugnaini M, Pasquini I, Rocchi S and Vignoli V 2011 Modeling of the influence of H_2O on metal oxide sensor responses to CO *Sensors Actuators* B **159** 82–91

[24] Tulzer G, Baumgartner S, Brunet E, Mutinati G, Steinhauer S, Köck A and Heitzinger C 2012 Inverse modeling of CO reactions at SnO_2 nanowire surfaces for selective detection *Procedia Eng.* **47** 809–12

[25] Tischner A, Maier T, Stepper C and Köck A 2008 Ultrathin SnO_2 gas sensors fabricated by spray pyrolysis for the detection of humidity and carbon monoxide *Sensors Actuators* B **134** 796–802

[26] Köck A, Tischner A, Maier T, Kast M, Edtmaier C, Gspan C and Kothleitner G 2009 Atmospheric pressure fabrication of SnO_2-nanowires for highly sensitive CO and CH_4 detection *Sensors Actuators* B **138** 160–7

[27] Ding J, McAvoy T J, Cavicchi R E and Semancik S 2001 Surface state trapping models for SnO_2-based microhotplate sensors *Sensors Actuators* B **77** 597–613

[28] Hahn S H, Bârsan N, Weimar U, Ejakov S G, Visser J H and Soltis R E 2003 CO sensing with SnO_2 thick film sensors: role of oxygen and water vapour *Thin Solid Films* **436** 17–24

[29] Higham D J 2008 Modeling and simulating chemical reactions *SIAM Rev.* **50** 347–68

[30] Morrison S R 1990 *The Chemical Physics of Surfaces* vol 1977 (New York: Plenum)

[31] Barsan N and Weimar U 2001 Conduction model of metal oxide gas sensors *J. Electroceram.* **7** 143–67

Chemical Sensors: Simulation and Modeling ed G Korotcenkov (New York: Momentum Press) pp 447–69